Anal. Chem. **1998,** *70,* 4645−4652

Accelerated Articles

Generation of Micrometer-Sized Patterns for Microanalytical Applications Using a Laser Direct-Write Method and Microcontact Printing

B. A. Grzybowski, R. Haag, N. Bowden, and G. M. Whitesides*

Department of Chemistry and Chemical Biology, Harvard University, 12 Oxford Street, Cambridge, Massachusetts 02138

This paper describes a procedure that allows the rapid generation of elastomeric masters for microcontact printing (μCP) and for a new variant of this technique: controlled sagging microcontact printing (CSμCP). Using a low-power laser (10 mW) operating at 532 nm, the desired pattern is ablated in a thin poly(methyl methacrylate) film doped with a dye (rhodamine B base). Subsequent pattern transfer into poly(dimethylsiloxane) (PDMS) produces an elastomeric stamp for either μCP or CSμCP. Printing on the surface of gold gives patterns (wires or trenches) with feature sizes as small as 5 μm (μCP) and trenches (but not wires) as smalll as 1 μm (CSμCP). The ability of this technique to generate functional systems was demonstrated with an array of gold minielectrodes printed on a silicon wafer and an array of chemical microreactors molded in PDMS. The performance of the electrode array was characterized using cyclic voltammetry with Ru(III)-$(NH_3)_6Cl_3$, as the substrate. Microreactors were used as vessels to grow crystals of KNO_3 with a narrow dispersion in sizes and with largest dimensions of $\sim$15 μm.

Microcontact printing[1,2] (μCP) is a useful technique for fabricating patterns. The stamps required in this technique are generated by casting poly(dimethylsiloxane) (PDMS) against a "master" consisting of a surface having the desired pattern in bas relief (low relief pattern on the surface). These masters are easily fabricated photolithographically in thin poly(methyl methacrylate) (PMMA) films supported on silicon wafers, provided the mask required for the photolithography is available. Unfortunately, generating new chrome masks is usually too slow and expensive to make this method practical for exploratory work requiring microfabrication. Methods of generating masters based on thermal dye fixation, such as photomicrolithography or thermal wax transfer,[3] have a relatively low resolution (tens of micrometers). As an alternative, we and others have developed a technique for generating masks that we call "rapid prototyping".[4] This technique uses high-resolution printing (widely available commercially in photoshops) to make photomasks. Rapid prototyping routinely generates patterns with lines of 50-μm width and can be extended with difficulty to 20-μm lines: it presently is not applicable for smaller lines. Rapid prototyping is useful for making stamps for certain types of microanalytical systems,[5−8] MEMS,[9,10] and optical devices,[11] but it is limited to relatively large features. We sought methods to generate the bas relief patterns needed to produce stamps for soft lithography that did not require the generation of conventional photomasks and that were capable of resolution higher than rapid prototyping. Among the techniques we have explored is laser ablation of thin polymer films.

(1) Wilbur, J. L.; Kumar, A.; Kim, E.; Whitesides, G. M. *Adv. Mater.* **1994**, *6*, 600−604.

(2) For a general review on soft lithography including μCP, see: Xia, Y.; Whitesides, G. M. *Angew. Chem., Int. Ed. Engl.* **1998**, *37*, 551−575. Xia, Y.; Whitesides, G. M. *Annu. Rev. Mater. Sci.* **1998**, *28*, in press.

(3) Gregory, P. *High Technology Applications of Organic Colorants*; Plenum Press: New York, 1991.

(4) Quin, D.; Xia, Y.; Whitesides, G. M. *Adv. Mater.* **1996**, *8*, 917−919.

(5) Petersen, K. E. *Proc. IEEE* **1982**, *70*, 420−457.

(6) Jacobson, S. C.; Hergenroder, R.; Koutny, L. B.; Ramsay, J. M. *Anal. Chem.* **1994**, *66*, 2369−2373.

(7) Hadd, A. G.; Raymond, D. E.; Halliwell, J. W.; Jacobsen, S. C.; Ramsey, J. M. *Anal. Chem.* **1997**, *69*, 3407−3412.

(8) General reviews and highlights of microanalytical systems: Service, R. E. *Science* **1995**, *268*, 26−27. Manz, A. *Chimia* **1996**, *59*, 140−145. Craston, D.; Cowen, S. *Chem. Brai.* **1996**, October, 31−33. Goffeau, A. *Nature* **1997**, *385*, 202−203. van der Berg, A., Bergveld, P., Eds. *Micro Total Analytical Systems*; Kluwer Academic Publishers: London, 1995.

(9) Bryzek, J.; Peterson, K. E.; McChulley, W. *IEEE Spectrum* **1994**, (Sept), 20.

(10) MacDonald, N. C. *Microelectron. Eng.* **1996**, *32*, 49−73.

(11) Lee, S. S.; Lin, L. Y.; Wu, M. C. *Appl. Phys. Lett.* **1995**, *67*, 2135−2137.

10.1021/ac9807621 CCC: $15.00
Published on Web 10/08/1998

Laser ablation is an accepted tool for the modification of polymer surfaces[12,13] and dopants, such as dyes, can enhance its efficiency.[14] Fabrication of patterns with feature sizes of several tens of nanometers has been reported.[15,16] These high-resolution direct-write processes, however, have the disadvantage of long processing times and limited process ranges, and they require expensive UV lasers and optical equipment. Here we describe a rapid and inexpensive benchtop technique for fabrication of PDMS stamps, beginning with laser ablation of dye-doped thin polymer films using a low-power visible laser. By making use of the specific topology of ablated lines to narrow these features when the stamp is in contact with the surface, this method yields features as small as 1 μm. With the stamps generated by this process, we fabricated several microstructures, including an array of gold microelectrodes and an array of microreactors, and demonstrated their use in microanalytical applications. The stamps generated by our method can be reused a number of times (more than 100) without loss of performance.

EXPERIMENTAL SECTION

Fabrication of Stamps for μCP. The polymer films were prepared by doping PMMA with rhodamine B base (Rh-B). Both reagents were purchased from Aldrich and used without further purification. Solutions of varying amounts of PMMA and Rh-6G in chloroform were prepared. They were sonicated for 5 min to facilitate dissolution of the dye and then centrifuged at 5*g* for 10 min to remove undissolved dye particles. Silicon wafers (2 in., Silicon Sense Inc.) were spin-coated with the solutions of polymer and dye. The content of both the dye and polymer in the spin-coating solution, and the spinning rate, were optimized (0.04 g of PMMA, 0.04 g of Rh-B, 1 mL of $CHCl_3$, 750 rpm/10 s) to yield uniform, smooth polymer layers with a thickness of ~6 μm.

A 10-mW diode-pumped Nd:YVO_4 laser (Brimrose, Baltimore, MD) operating at $\lambda = 532$ nm was used for laser ablation. For the generation of the microstructure, the polymer-coated silicon wafer was placed on an *XY*-motorized translational stage (1-μm precision; Edmund Scientific, Barrington, NJ). The position of the stage was adjusted so that the laser beam was focused through a microscope objective (40× or 80×) 3−4 μm into the surface of the polymer layer. By moving the translational stage, the desired patterns could be ablated in the polymer film.

The silicon wafer containing the microstructure was subsequently used as a master to fabricate an elastomeric stamp for μCP (Figure 1). PDMS (Dow Corning) was cast on the master and thermally cured for 1 h at 75 °C. The PDMS was then gently peeled off, washed with ethanol, and dried. The resulting stamp was used for μCP as described previously.[1,2]

Fabrication of Stamps for Controlled Sagging μCP (CSμCP). A pattern was ablated in PMMA/Rh-B film through an 80× objective, with a laser power of 10 mW and at a laser scan rate of 50 mm/min. A PDMS stamp was fabricated as described above and was subsequently used as a master. Its surface was cleaned and oxidized in an oxygen plasma cleaner (PDC-23G, Harrick) for 10 s and then silanized for 1 h with (tridecafluoro-1,1,2,2-tetrahydrooctyl)-1-trichlorosilane.[17] PDMS was cast against this stamp and thermally cured at 75 °C for 1 h. The master and the cured replica were then cut out of the bulk polymer using a razor blade and gently separated to give a stamp for CSμCP (Figure 2).

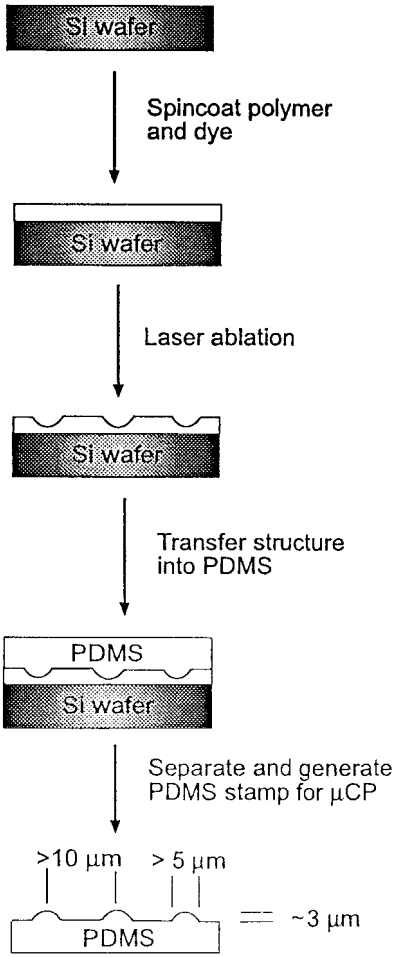

Figure 1. Stamp preparation by laser ablation for microcontact printing.

Pattern Transfer and Etching. The surface of the PDMS stamp was wetted with a 2% solution of hexadecanethiol in ethanol and the pattern stamped onto a gold surface (5 nm of titanium adhesion layer, 38 nm of gold), supported on either a glass plate or a silicon wafer.[2] Selective etching was done with ferri/ferrocyanide etchant[18] for 13 min. The composition of the etchant was $K_2S_2O_3$ (0.1 M), $K_3Fe(CN)_6$ (0.01 M), and $K_4Fe(CN)_6$ (0.001 M). *Caution: Potassium ferricyanide is light sensitive. The photodecomposed products contain free cyanide ion. Potassium ferricyanide is also incompatible with acids and releases HCN. Conduct the procedures in a well-ventilated hood and avoid prolonged exposure of potassium ferricyanide to light.*

Microfabrication of a Minielectrode Array and Cyclic Voltammetry. The gold electrode array was fabricated by a two-

(12) Roberts, M. A.; Rossier, J. S.; Bercier, P.; Girault, H. *Anal. Chem.* **1997**, *69*, 2035−2042.
(13) Srinivasan, R.; Baren, B. *Chem. Rev.* **1989**, *89*, 1303−1316.
(14) Lippert, T.; Yabe, A.; Wokaun, A. *Adv. Mater* **1997**, *9*, 105−119.
(15) Kim, D. Y.; Tripathy, S. K.; Li, L.; Kumar, J. *Appl. Phys. Lett.* **1995**, *66*, 1166−1668.
(16) Mullenborn, M.; Dirac, H.; Petersen, J. W. *Appl. Phys. Lett.* **1995**, *66*, 3001−3003.
(17) Chaudhury, M. K.; Whitesides, G. M. *Langmuir* **1991**, *7*, 1013−1025. Chaudhury, M. K.; Whitesides, G. M. *Science* **1992**, *255*, 1230−1232.
(18) Xia, Y.; Zhao, X.-M.; Kim, E.; Whitesides, G. M. *Chem. Mater.* **1995**, *7*, 2332−2337.

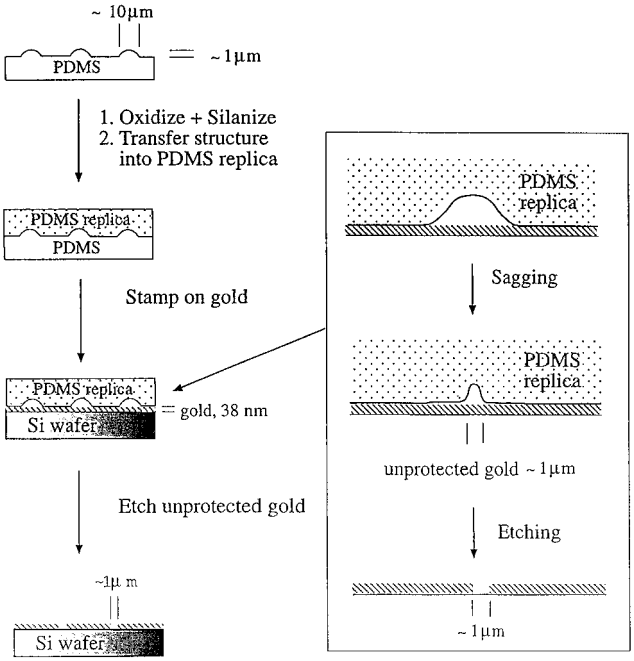

Figure 2. Steps involved in using controlled sagging microcontact printing for generating 1-μm features. The pattern is transferred from a PDMS stamp prepared by laser ablation into a PDMS replica. This replica is used for stamping onto a gold surface, and the unprotected gold is removed by etching to give features of sizes of ~1 μm.

step μCP process. First, the array of lines was stamped with a stamp fabricated as described above. Next, the electrical connections were stamped to connect the "loose" ends on each side of the electrode array with an easily addressable contact pad. Selective etching of the unprotected gold gave a minielectrode array with electrode width of ~10 μm and spacing of ~30 μm.

The electrochemical measurements were made with an AFCBP1 biopotentiostat (Pine Instruments, PA) interfaced to a personal computer. A small PDMS ring with an inner diameter of ~1 mm was placed on top of the Au minielectrode array. The resulting well contained the aqueous redox solution. The reference electrode, Ag/AgCl in saturated KCl solution (Ag/AgCl/KCl; Bioanalytical Systems, West Lafayette, IN) was placed inside the PDMS ring, ~1 mm away from the electrode array on the glass surface. An aqueous solution of hexaammineruthenium(III) chloride (0.5 and 1 mM,) and lithium perchlorate (0.1 M) were used as the redox/electrolyte solution. Prior to the measurement, the electrolyte was purged with argon. Cyclic voltammetry was performed at 100, 200, and 400 mV/s.

Crystallization in Microreactors. A saturated solution of KOH in anhydrous ethylene glycol (both reagents were purchased from Aldrich) was prepared and applied on a PDMS stamp having an array of microwells on its surface. The liquid was drained off the surface using a pipet, so that only the wells remained filled with the solution. Upon exposure of this array to the vapor of fuming nitric acid (99%, Aldrich), crystals of KNO_3 were obtained in the wells. To achieve monodispersity (i.e., one crystal per well, all crystals of approximately same size), recrystallization was performed by blowing moist air onto the surface.

RESULTS AND DISCUSSION

Fabrication of Stamps and μCP. For laser ablation to be efficient, the frequency of the laser must approximately match the wavelength of maximum absorption of the dye dopant in the polymer film. Rhodamine B base was chosen because its wavelength of maximum absorption (λ_{max} = 543 nm) is close to the wavelength of a laser we used (λ = 532 nm). In addition, Rhodamine B base is easily soluble in common organic solvents such as dichloromethane, chloroform, and ethyl acetate. We used these three solvents in combinations with common polymers (polystyrene (PS), polyurethane (PU; Norland Optical Adhesive 71), PMMA, and poly(vinylene chloride) (PVC) to identify the best composition for a spin-coating solution (Table 1).

Table 1. Properties of Polymer–Solvent Systems in Spin-Coating and Laser Ablation[a]

	solvent		
polymer	CH_2Cl_2	$CHCl_3$	CH_2Cl_2/AcO
PS	− −	− −	− −
PU	+ −	+ −	− −
PMMA	− +	++	− +
PVC	− −	− −	− −

[a] The first characterization describes the smoothness of the spin-coated film (+ smooth, − rough). The second characterization gives the efficiency of laser ablation (+ deep lines, − shallow lines).

To fabricate stamps of high quality, the polymer layer used to generate the master had to meet three requirements. First, the spin-coated film had to be very smooth. Second, the polymer film had to be highly absorptive to ablate satisfactorily under the influence of the low-power laser. Third, the thickness of the film had to be greater than ~3 μm to yield a useful aspect ratio in the patterns that were generated. Only the PMMA/$CHCl_3$ solution met the first two conditions. To satisfy the third requirement, the spin-coating procedure was optimized to a spin rate of 750 rpm and a spinning time of 10 s.

Figure 3 shows the shapes of the features produced by ablation in the optimized Rh-B/PMMA film. Representative line profiles of the masters were shallow, curved domes, 3 μm deep, with a half-width of ~5 μm. These lines produced stamps with complementary shapes. The topographies of ablated features depended not only on the composition of the polymer film but also on the speed used to write the patterns. We examined lines generated at various drawing speeds by SEM and AFM. Ablating at lower speeds gave better results than at higher speeds: the optimum (performance vs time) ablation scan rate in our experiments was ~10 mm/min; for faster ablation rates, the lines were too shallow to be useful for subsequent stamping. Figure 3 shows the SEM (a, b) and AFM images (c) of a line generated at 10 mm/min scan rate. The bumps at the bottom of the trench do not exceed 100 nm. We do not expect surface imperfections of this size to decrease the quality of the printing of micrometer-sized features.

The width of the features generated by laser ablation depends also on the diameter of the laser beam in the focal point and the position of the focal point. When an 80× objective was used to focus the laser beam, the lines made by stamping were 5 μm wide. With a 40× objective the width increased to 10 μm and with a 20× objective they had widths of 20 μm. The best aspect ratios of the ablated features were obtained with the laser beam focused 3−4 μm into the polymer film (focusing at the surface gave shallower and broader lines). This effect results from maximiza-

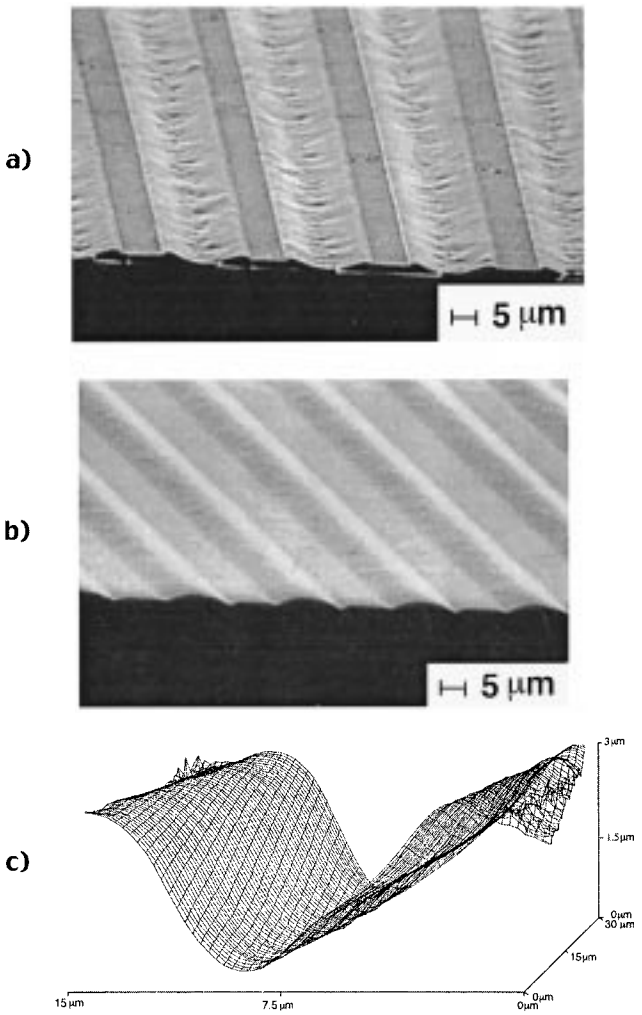

Figure 3. SEM images of (a) lines generated by laser ablation in a PMMA/Rh-6B base film and (b) the PDMS replica from this master. (c) is the AFM image of an ablated line in PMMA/Rh-6B. Features were ablated through a 80× objective with laser scan rate of 10 mm/min and laser power of 10 mW.

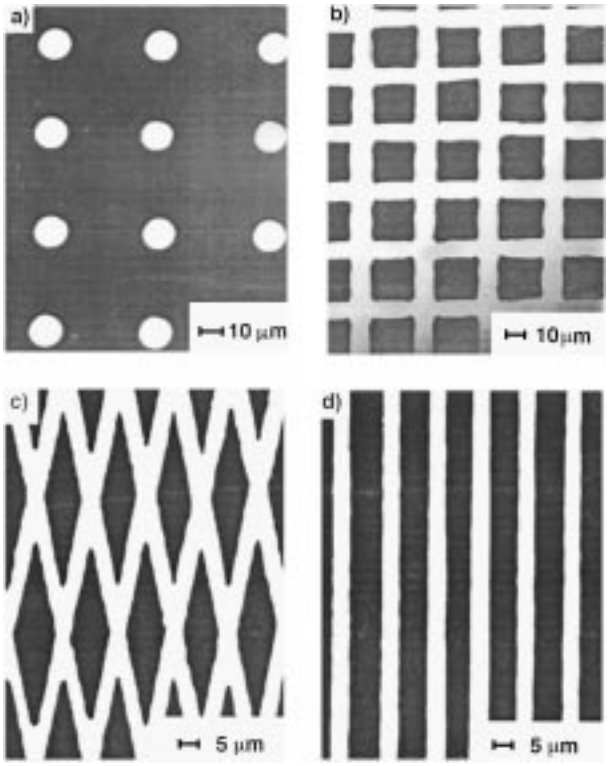

Figure 4. Optical micrographs showing representative patterns. The patterns were generated by stamping hexadecanethiol onto a gold surface, followed by selective etching of gold. White regions correspond to unetched gold. Pattern c was obtained by stamping parallel lines twice, with an angle of ~30° between the two impressions. Stamps used in generating these patterns were obtained via ablation through either a 40× (a, b) or an 80× (c, d) objective and with a laser scan rate of 10 mm/min and laser power of 10 mW. A solution of hexadecanethiol in methanol (2 mM) was used for stamping.

tion of the energy density in the polymer film, which in turn determines the rate of the thermal degradation of the polymer/dye matrix.

Having identified the experimental conditions that resulted in effective ablation, we generated several masters with various patterns: an array of 10-μm circular dots, an array of 5-μm lines, and an array of squares. A single dot was obtained by point irradiation of the film for 1 s. The laser shutter was then closed, the translational stage was moved to the next position on the grid, and the process was repeated. The patterns of lines were fabricated using the procedures (40× or 80× objective, 10 mm/s) described earlier. Once the masters were prepared, they served as templates for preparation of elastomeric stamps; the procedures for this pattern transfer have been described.[1,2] After stamping on a thin gold surface, selective etching yielded patterns shown in Figure 4. The feature size after microcontact printing is smaller than the feature size of the master (Figure 2) by the factor of ~2. This difference is expected: the features produced by ablation (trenches ablated in the polymer film) have a "bell" shape—that is, wider at the surface of the polymer film, shallower at its bottom (see Figure 1). When this shape is transferred into the stamp, and then microcontact printed onto a gold film, only the narrower part of the "bell" comes in contact with the surface of the metal. Because the same process produces the profiles of all features in a single master, the pattern that results in the etched metal film is also uniform in size. This patterning procedure is fully successful only if the separation of ablated features is greater than or equal to the feature size (for instance, 5-μm lines should be separated by at least 5 μm). Below this limit, the ablated "bell"-shape line profiles overlap, and the aspect ratio in the features on the stamp becomes too small to give selective pattern transfer.

The stamps generated by this technique can be reused many times (more that 100) without loss of performance. Because PDMS resists most chemicals, stamps can be stored for prolonged periods of time. When fabricating complex patterns, one should consider whether ablation of an entire pattern is necessary: successive stamping with simpler patterns might suffice (Figures 4c and 7). Because laser ablation is a serial process, this technique might not be well suited for fabrication of stamps of large areas: generating a 1-cm^2 pattern with 5-μm features and with 50% of the surface of the polymer ablated would take more than 10 h. Such large areas are, however, seldom needed for microanalytical applications and even when they are, the reusability of stamps (once they have been prepared) makes this time scale relative. The sensitivity of the system (~1 kJ/cm^2) is low compared to that of classical PMMA positive photoresists used in photolithography (~100 mJ/cm^2).[19−22] The technique, however,

does not require that a chrome mask be available, nor that the procedures be carried out under cleanroom conditions. The low cost of the equipment that is required and flexibility in design of stamps make it an alternative to photolithographic techniques for certain simple patterns and for exploratory pattern development where rapid turnaround is required.

Controlled Sagging μCP. The lower limit for the size of the features generated by the laser ablation/stamping technique described here is 5 μm. With the aim of achieving higher resolution, we developed a variant of this method that is capable of producing 1-μm features (Figure 2). The method starts with generation of a PDMS stamp as described earlier, but at higher laser scan rates (~50 mm/min) so that the features in the stamps have low aspect ratios (1:10). The pattern is transferred from the PDMS stamp into a PDMS replica. This replica has a positive image of the originally ablated pattern embossed on its surface. The replica is subsequently used for stamping hexadecanethiol onto a gold surface. During stamping, the sides of the grooves sag and touch the surface of gold:[23] only the middle part of the groove (around the "apex") does not come in contact with the surface and only a thin slice of the gold surface below the groove is not protected by the stamped SAM. When selective etching is done, gold is removed only from this unprotected region. This process gives 1-μm-wide features reproducibly. Figure 5 shows an array of 1-μm lines generated by this procedure. We hypothesize that the size of these lines is determined primarily by the contour of the stamp, the mechanical properties of PDMS, and the surface free energy of the gold film.

The sagging observed during μCP could be caused either by the pressure exerted by the stamp on the features in the bas relief or by "capillary-like" spreading of PDMS into contact with the gold.[17] In the first case, the bulk PDMS presses on the features in the bas relief: the regions near the edges are pushed down toward the gold surface before the regions near the center (near the "apex"). The edge regions of the features are less curved than the middle ones: the middle part resembles a "dome", more unyielding to squeezing than a "flat roof" near the edge. If this description were correct, one would expect more sagging (and subsequently smaller features after printing) if additional pressure—in excess of the pressure exerted by the stamp itself—were applied to the stamp during μCP. We tested this hypothesis experimentally by placing calibrated weights on top of the stamp during μCP. For small pressures (<10 Pa at the interface between the stamp and gold), the width was not reduced (but the roughness of the edges increased considerably); for higher pressures, the features sagged completely and no features were observed after etching. We also observed that when the features were surrounded by PDMS from all sides (closed channels, separated dots, etc.), the width actually increased with increased pressure.

If the hypothesis of "capillary-like" sagging were correct, the performance of CSμCP should decrease if contaminated/old gold was used as the substrate for stamping, since the surface of contaminated gold is covered with a hydrocarbon film and has a low solid–vapor interfacial energy. The increase in the width of the stamped features to ~5 μm when 3-month-old gold was used suggests that the sagging is, indeed, caused by capillary-like effects.[24] We corroborated this hypothesis with a qualitative finite element modeling (FEM).[25] Favorable energy (~20 ergs/cm^2 [17]) was assigned to PDMS spreading on gold, and the total energy of the system was minimized. Figure 6 shows the stages during sagging modeled by FEM.

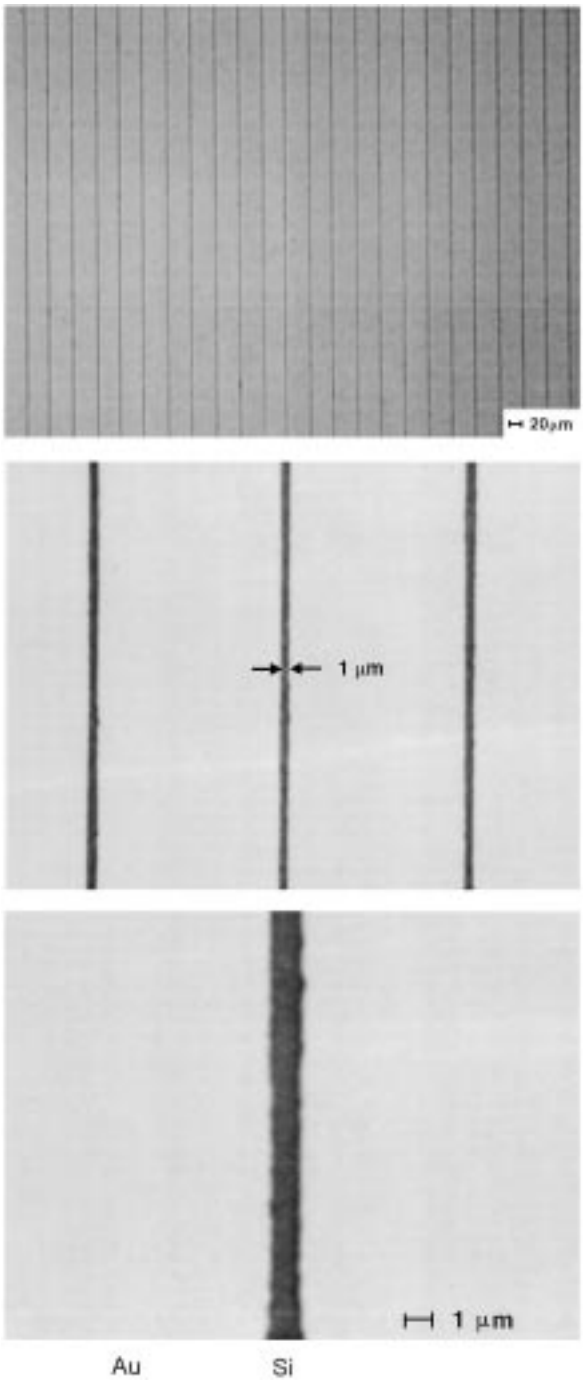

Figure 5. Optical micrograph of a pattern of parallel lines of 1-μm width etched in gold. The pattern was generated by controlled sagging microcontact printing on a gold-covered silicon wafer using a solution of hexadecanethiol (2 mM in methanol) to ink the stamp, followed by selective etching of the unprotected gold. White regions correspond to the unetched gold, and dark regions correspond to silicon.

(19) Van Pelt, P. *SPIE Proc.* **1981**, *275*, 150.
(20) Wilkins, C.; Reichmanis, E.; Chandross, E. *J. Electrochem. Soc.* **1980**, *127*, 2510–2513.
(21) Wilkins, C.; Reichmanis, E.; Chandross, E. *J. Electrochem. Soc.* **1982**, *129*, 2552–2555.
(22) Tsuda, M.; Nakamura, Y.; Oikawa, S.; Nagata, H.; Yakota, Y.; Nakane, H.; Tsunori, T.; Nakase Y.; Mifusi, T. *Photogr. Sci. Eng.* **1979**, *23*, 290–294.
(23) Biebuyck, H. A. *IBM J. Res., Dev.* **1997**, *41*, 159–167.

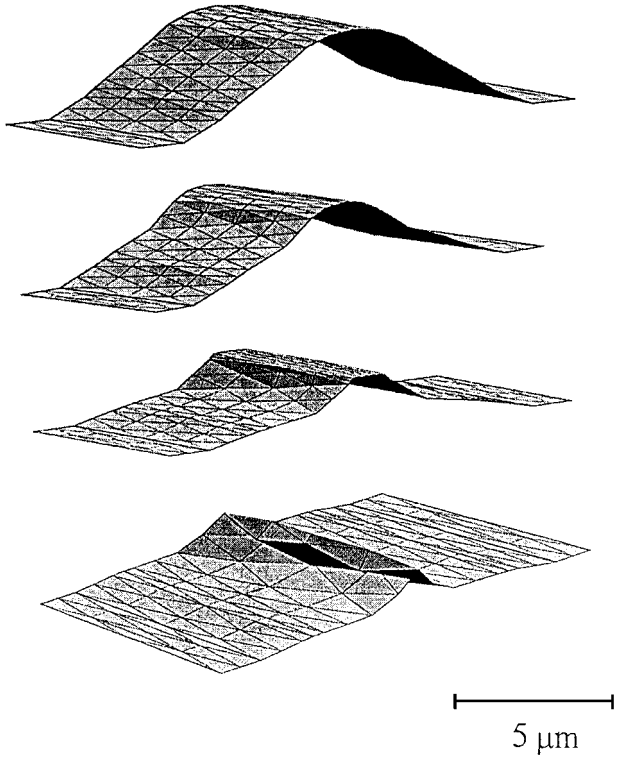

Figure 6. Sagging of the bas relief features during controlled sagging microcontact printing. The sagging of a typical feature (a line) was modeled using the finite element method. Only the surface of PDMS is shown. The sketches show various stages during the energy minimization procedure. The values of the density of PDMS (1.05 g/cm^3) and its Young's modulus (20 MPa) used in the calculations were obtained from the manufacturer's technical specification sheet (Dow Corning). The energy gain from the spreading of the SAM-covered PDMS on gold was assigned the value 20 ergs/cm^2.

More control over the sagging process could be realized if the cross section of the features in the stamp was tailored with grater precision via conventional micromachining methods. One appealing possibility would be to fabricate features of triangular cross section, with the hypothenuse acting as a sagging membrane.

The patterns generated by our method can be used in two ways: to produce either small features (1 μm) separated by relatively large distances (>20 μm) or, conversely, large features separated by small distances. The first strategy could be useful in microfluidic devices:[26] after etching away the unprotected gold, the bare silicon regions can be further etched to produce microchannels[27] for flow cells,[28] electrophoresis systems,[29] rectifiers,[30] or microfluidic logic devices.[31] The relatively high speed of laser ablation in this technique would allow for fabricating long channels in short times. This method might also lead to IR filters and polarizers.[32] Large features separated by small distances might be useful in fabricating arrays of tiltable structures such as cantilevers[33] if the silicon were underetched below the SAM protected gold layer.

Microanalytical Applications. To demonstrate possible applications of these techniques in microanalytical applications, we fabricated two functional systems: an array of gold minielectrodes printed on a silicon wafer and an array of microwells for crystallization.

Owing to the small separation of working and counter electrodes, the minielectrode array[34] offers several advantages over macrosized electrodes. For example, the resistance of the cell is small due to the short distance between the electrode surfaces and hence can be used with high resistivity media. The total area consumed by one minielectrode array is only ~2 mm^2, and hence ~900 such devices can be placed on a 2-in. silicon wafer. Common techniques for fabrication of minielectrodes include photolithography,[35] CVD,[36] and micromolding,[37] among others.

To produce the array of minielectrodes, we first fabricated a stamp for μCP having an array of lines embossed on its surface using the method described earlier (40× objective, total ablation time of 90 min). This pattern was stamped onto a gold-covered silicon wafer (Figures 7 and 8). Electrical connection of the ends on the outside of the pattern was accomplished by μCP in a separate step using a rectangular (5 × 20 mm) PDMS stamp. Removal of the gold unprotected by SAMs by etching gave the desired structure. The resulting electrode array was free of shorts, as confirmed by a very large electrical resistance between counter and working electrodes. A PDMS ring of inner diameter ~1 mm was placed on top of the minielectrode array (Figure 7) and filled with a test solution (1 mM $Ru(NH_3)_6Cl_3$ in aqueous 0.1 M $LiClO_4$ solution). A reference electrode (Ag/AgCl/KCl) was dipped into

(24) Reactive spreading across the surface and through the vapor phase also shrinks the size of the features. This effect, however, is important only in the region near the edges of the features, where the distance between the surface of the stamp and gold is on the order of hundreds of nanometers and cannot account for the transport of thiol into the center of the feature where the distance is ~2 μm. Moreover, the stamping time in our experiments (~10 s) is much shorter than that in the experiments where reactive spreading was important. For more discussion, see: Xia, Y.; Whitesides, G. M. *J. Am. Chem. Soc.* **1995**, *117*, 3274−3275. Delamarche, E.; Schmid, H.; Bietsch, A.; Larsen, N. B.; Rothuizen, H.; Michel, B.; Biebuyck, H. *J. Phys. Chem. B* **1998**, *102*, 3324−3334.

(25) The name of the public domain computer code used for FEM is Surface Evolver. It is under development by K. A. Brakke as a part of the Geometry Center, University of Minnesota, which is sponsored by the National Science Foundation and the Minnesota Supercomputer Center. Further details can be found in the Surface Evolver manual. For background reading on FEM, see: Hughes, J. R. *The Finite Element Method. Linear Static and Dynamic Finite Analysis*; Prentice-Hall: Englewood Cliffs, NJ, 1987. Burnett, D. S. *Finite Element Analysis. From Concepts to Applications*; Addison-Wesley: Menlo Park, CA, 1987.

(26) For examples of micromachined microfluidic devices, see: Kovacs, G. T. A. *Micromachined Transducers*; WCB/McGraw-Hill: New York, 1998; pp 779−899.

(27) Lammerink, T. S. J.; Tas, N. R.; Berenschot, J. W.; Elwenspoeck, M. C.; Fluitman, J. H. *Proceedings of the IEEE 1995 Micro Electro Mechanical Systems Workshop (MEMS 95)*, Amsterdam, The Netherlands, Jan 29−Feb 2, 1995; pp 13−18.

(28) Sobek, D.; Senturia, S. D.; Gray, M. L. *Proceedings of the Solid State Sensor and Actuator Workshop*, Hilton Head Island, SC, June 13−16, 1994; pp 260−263.

(29) Harrison, D. J.; Glavina, P. G.; Manz, A. *Sens. Actuators B* **1993**, *10*, 107−116.

(30) Humphrey, E. F., Tarumoto, D. H., Eds. *Fluidics*; Fluid Amplifier Associates: Boston, 1965.

(31) Foster, K.; Parker, G. A. *Fluidics: Components and Circuits*; Wiley-Interscience: New York, 1970.

(32) Ohnstein, T. R.; et al. *Proceedings of the Solid State Sensor and Actuator Workshop*, Hilton Head Island, SC, June 3−6, 1996; pp 196−199.

(33) Petersen, K. E.; et al. *Proceedings of the Solid State Sensor and Actuator Workshop*, Hilton Head Island, SC, June 6−9, 1988; pp 144−147.

(34) Wang, D. L.; Heller, A. *Anal. Chem.* **1993**, *65*, 1069−1073. Katakis I.; Heller, A. *Anal. Chem.* **1992**, *64*, 1008−1013.

(35) Kakerow, R.; et al. *Sens. Actuators A* **1994**, *43*, 296−301.

(36) Cooper, J. B.; Pang, S.; Albin, S.; Zheng, J.; Johnson, R. M. *Anal. Chem.* **1998**, *70*, 464−467.

(37) Zhang, X.; Ogorevc, B. *Anal. Chem.* **1998**, *70*, 1646−1651.

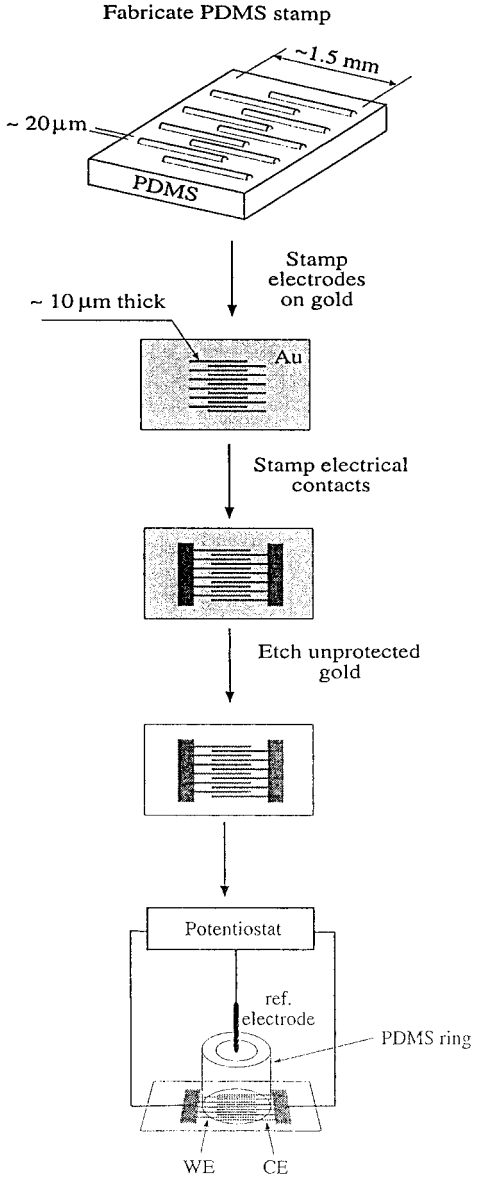

Figure 7. Fabrication of the array of planar minielectrodes on a Si/SiO_2 surface and the experimental setup used for cyclic voltammetry (CE, counter electrode; WE, working electrode).

the solution in the PDMS ring, and cyclic voltammetry was performed. Figure 9 shows cyclic voltammograms obtained for three different voltage scan rates. The curves show clear oxidation and reduction waves with an experimentally determined redox potential $E_{1/2} = -0.16$ V, which is in good agreement with reported measurements under similar conditions.[38] The observed peaked response at slow voltage scan rates and the increase in Faradaic current with increasing voltage scan rate (Figure 9) are typical of a minielectrode rather than a microelectrode.[39] This behavior is expected: electrodes whose thickness (width of a single wire in our device) is in the micrometer range, but whose length is on the order of millimeters, do not exhibit the steady-state responses and reduced Ohmic effects typical of microelectrodes. The

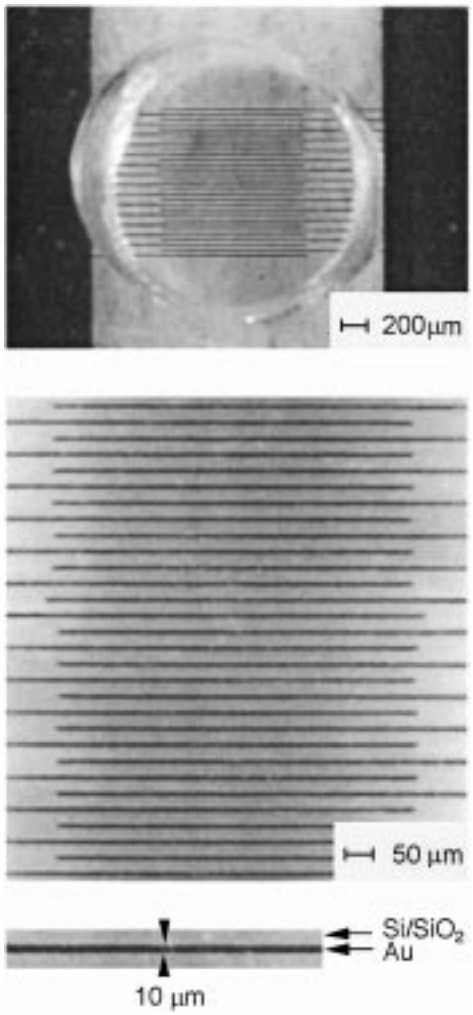

Figure 8. Optical micrographs of the array of gold minielectrodes printed on a Si/SiO_2 wafer. Solution of hexadecanethiol (2 mM in ethanol) was used in printing the pattern. Dark regions correspond to gold. The electrode pattern was ablated through a 40× objective.

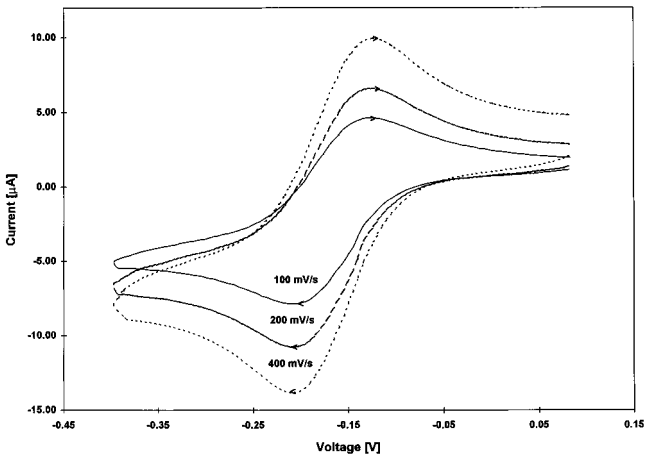

Figure 9. Cyclic voltammograms of an aqueous hexaammineruthenium(III) chloride (1 mM) and lithium perchlorate (0.1 M) solution at three different sweep rates, recorded with the array of gold minielectrodes (total electrode area, ~0.25 mm^2).

(38) Muskal, N.; Turyan, I.; Shurky, A.; Mandler, D. *J. Am. Chem. Soc.* **1995**, *117*, 1147−1148.

(39) Fleischmann, M.; Pons, S.; Rolison, D. R.; Schmidt, P. *Ultramicroelectrodes*, Datatech Systems, 1987. Ammann, D. *Ion-selective Microelectrodes: Principles, Design and Application*; Springer-Verlag: Berlin, 1986. Gnetov, A. V. *Stekliannye Mikrolektrody*; Nauka: Leningrad, 1986. Standen, N. B., Gray, P. T. A., Whitaker, M. J., Eds. *Microelectrode Techniques: The Plymouth Workshop Handbook*; The Company of Biologists Ltd.: Cambridge, 1987. Foster, R. J. *Chem. Soc. Rev.* **1994**, *201*, 289−297.

diffusion field in our device is linear, in contrast to hemispherical diffusion fields in microelectrodes. The lower detection limit of our device (visible Faradaic currents) is ~0.5 mM $Ru(NH_3)_6Cl_3$ in 0.1 M $LiClO_4$ electrolyte solution.

In the second application we fabricated an array of microscopic vessels (which we call microreactors to emphasize their use as containers for chemical processes) and performed parallel crystallization in them. The ability to perform many chemical reactions at the same time and on the same (preferably small) scale is one of interest in a number of fields. Arrays of microscopic vessels are well suited for this purpose and can be used in, for example, combinatorial chemistry[40] and for studying statistical events such as nucleation of crystals and formation of drops of condensed liquids.[41] We have recently described a photolithographic method of fabricating large arrays of microreactors;[42] more details on the applications of these structures can be found in that paper.

In this work, we generated arrays of ~1000 microreactors (~20 μm in diameter, separated by ~20 μm) using the laser direct-write method. The fabrication started with ablating an array of dots in the polymer film. This pattern was transferred into a PDMS stamp to give a pattern of microposts. By molding against this structure, we generated a PDMS replica with microreactors ("wells") embossed on its surface (Figure 10). We demonstrated crystallization in these microreactors. A saturated solution of KOH in ethylene glycol[43] was delivered to the wells by a discontinuous dewetting.[43] Exposure of the reactors to a vapor of fuming nitric acid precipitated crystals of KNO_3 in the wells. To achieve monodispersity (that is, one crystal per well in uniformly sized wells), moist air was blown onto the surface, so that recrystallization could occur and small crystals could ripen into bigger ones. Figure 9a shows an optical micrograph of microreators having one crystal in each well. The uniformity in size is evident in those crystals having the same orientation.

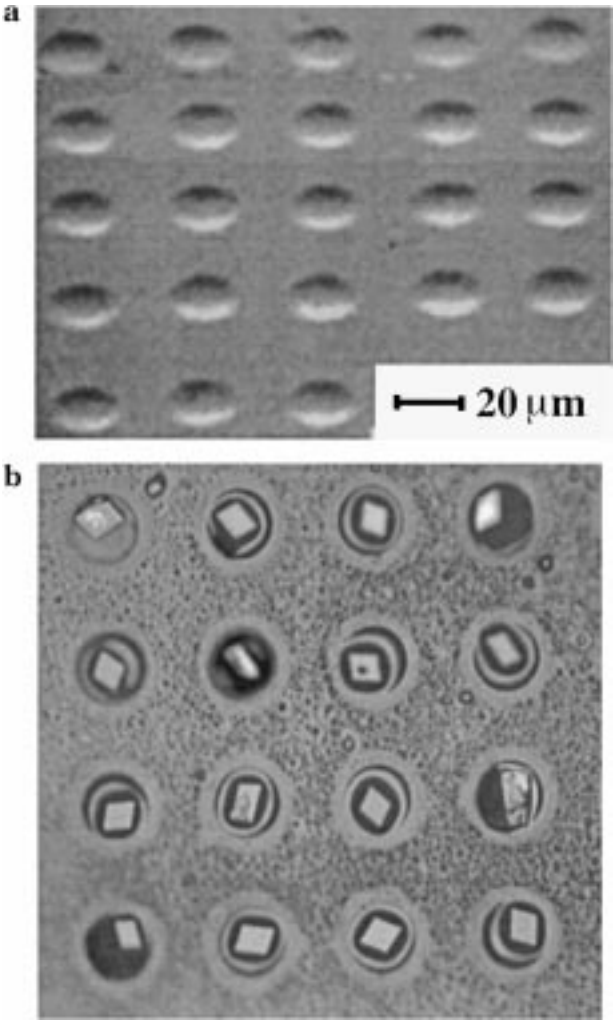

Figure 10. Crystallization in microreactors. (a) shows an SEM image of the array of microreactors; (b) is an optical micrograph of an array of microreactors containing one crystal of KNO_3 per well. The wells were obtained by ablating through a 40× objective and subsequent pattern transfer into PDMS and then into a PDMS replica.

CONCLUSIONS

Laser ablation is the basis of a technique that allows the rapid and inexpensive fabrication of PDMS stamps for μCP and CSμCP with features down to 5 and 1 μm, respectively. None of the operations described (spin-coating, laser ablation, stamp generation, and microcontact printing) requires cleanroom conditions. Since this is a direct-write method, no specialized photolithographic equipment is required. The method is capable of creating arbitrary patterns under computer control and can generate simple patterns under manual control. The stamps generated by this method can be used to prepare devices and structures for microanalytical applications. An array of minielectrodes and an array of microreactors have been manufactured using this method; the total time required to generate each of these structures was less than 5 h. We believe that because of the simplicity with which it can generate simple patterns, its reliability, and its low cost, this procedure could be a useful alternative to conventional photolithographic techniques for generating elastomeric pattern-transfer elements for soft lithography.

ACKNOWLEDGMENT

This work was supported by the Defense Advanced Research Project Agency (DARPA) and by the National Science Foundation (NSF) under award ECS-9729405. This work made use of MRSEC Shared Facilities supported by the National Science Foundation under Award DMR-9400396. R.H. thanks the Deutsche Forschungsgemeinschaft for financial support.

Received for review July 13, 1998. Accepted September 9, 1998.

AC9807621

(40) You, A. J.; Jackmann, R. J.; Whitesides, G. M.; Schreiber, S. I. *Chem. Biol.* **1997**, *4*, 969−975.
(41) Biebuyck, H. A.; Whitesides, G. M. *Langmuir* **1994**, *10*, 2790−2793.
(42) Jackmann, R. J.; Duffy, D. C.; Ostuni, E.; Willmore, N. D.; Whitesides, G. M. *Anal. Chem.* **1998**, *70*, 2280−2287.
(43) Although PDMS is swollen by many organic solvents, it is unaffected by water, polar solvents (such as ethylene glycol) and perfluorinated compounds. For more detailed discussion, see ref 16.